Thermal boundary conductance to a two-dimensional helium film

J. E. Rutledge* and J. M. Mochel
Physics Department and Materials Research Laboratory, University of Illinois at Urbana-Champaign, 1110 W. Green Street, Urbana, Illinois 61801
(Received 23 January 1984; revised manuscript received 23 April 1984)

The thermal boundary conductance between vitreous quartz and a thin, superfluid helium film has been measured for the first time using third-sound resonance. This conductance, K_B, can be described as $0.25\times10^{-4}T^{6.3\pm1.0}$ W/cm^{2}K, between 0.7 and 0.1 K. Both the temperature dependence and magnitude preclude any bulk, acoustic-mismatch explanation. Three-phonon processes which conserve both energy and momentum produce a T^7 temperature dependence. It is concluded that the heat-transport mechanism must involve the solid helium layer as an intermediate. At low temperatures the third-sound resonance Q saturates, becoming temperature independent below 0.4 K. To explain this behavior an additional parameter, Γ, which characterizes intrinsic dissipation in a flowing film, must be added to the two-dimensional hydrodynamics. The low-temperature value of Γ decreases from 1.6 sec^{-1} for a 1.35-layer film to 0.4 sec^{-1} for a 4.40-layer film.

I. INTRODUCTION

The thermal boundary conductance between a solid and liquid helium can usually be understood in terms of the transmission of phonons. Generally, above 0.1 K, the experimental conductance is at least a factor of 10 larger than predicted by the acoustic-mismatch theory[1] first proposed by Khalatnikov. It has become clear that nonlinear scattering processes at the interface must be considered with all the attendant problems of detailed mechanisms and mode conversion.[2] It has been demonstrated experimentally[3] that much of the anomalous transmission observed is due to "dirty" surfaces. However, such reflection experiments are insensitive to surface processes once the phonon transmission falls below a few percent. Multiphonon processes can be discussed phenomenologically[4] and of course can provide a qualitative understanding of additional phonon transmission.

We have suppressed ordinary (Kapitza) single-phonon processes by reducing the thickness of the superfluid helium phase to a few monolayers. We are essentially measuring the Kapitza boundary conductance between the substrate and a two-dimensional superfluid. For a phonon to have a wave vector perpendicular to the interface, in the superfluid phase, would require its energy to be in excess of 10 K. Two phonon processes are possible (a substrate phonon excites a local surface state which reradiates a new excitation parallel to the surface) and have been considered below but are not seen experimentally. This may be due to the locally smooth substrate of crystalized argon, as described in the next section, which buries such surface states. We are able to measure the boundary resistance in this system through the use of third-sound resonance.[5] Both the resonant linewidth and the coupling to the generator and detector are established by this boundary resistance. Another mode of dissipation in thin helium films, seen in the heat-pulse experiments of Guo and Maris,[6] is due to the expulsion of atoms from the film into the gas phase.[7] Since we are measuring close to equilibrium and below 0.7 K, where there is no significant vapor phase, this mode of dissipation is not important.

In the next section, a detailed description of the third-sound resonator and experimental procedures will be given. A detailed thermal analysis of the cell—helium-film system follows and is carried out to correctly obtain the magnitude of the boundary resistance. However, the most striking feature of these measurements, the large temperature dependence and small magnitude of the boundary conductance, appears even in the raw data. In fact, below 0.1 K, the superfluid surface wave thermal relaxation time becomes sufficiently long to prevent its observation.

Another feature of the data is the saturation of the resonance Q. Below 0.4 K, the Q has a temperature-independent value of the order of 10^4 for all but the thinnest films. Values of the Q calculated from the K_B values needed to explain the resonance amplitude are 3 orders of magnitude too larger at 0.15 K. Therefore, we have included a second parameter, Γ, in the third-sound equations to account for the Q saturation. Numerical values of Γ are derived from the data. After the analysis of the data we consider various models which involve two- and three-phonon scattering.

II. THIRD-SOUND RESONANCE CELL

A third-sound resonance cell is a vitreous quartz envelope with its inside surfaces coated by approximately 15 atomic layers of solid argon. The helium film under study is adsorbed on the argon. The argon determines the van der Waals binding of the helium,[8] and consequently the third-sound velocity,[5] but the quartz dominates the heat capacity and thermal conductivity of the substrate.[9] The cell is shown in cross section in Fig. 1. The ac power from the heater excites a temperature oscillation, through the 100-μm quartz wall, in the helium film. Due to the thermomechanical effect, the superfluid component of the helium film is set in motion. The resultant film thickness

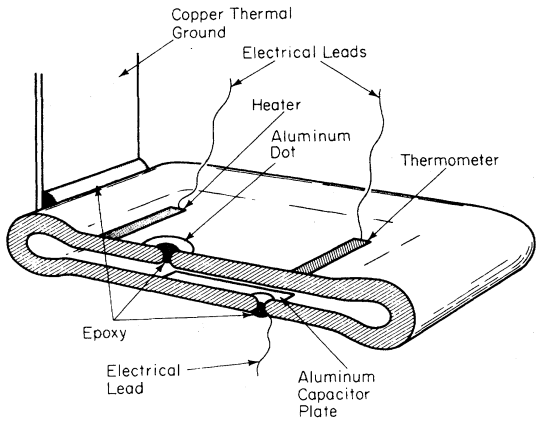

FIG. 1. A third-sound resonator. The thickness is exaggerated for illustration. The internal dimensions are $0.6\times1.8\times10^{-3}$ cm^3. Helium is passed through the walls by diffusion at room temperature and below 1 K the helium coats the inner surface to produce a closed superfluid film. The fundamental resonance corresponds to the film sloshing back and forth from one end of the cell to the other.

wave propagates around the inner surface of the cell. The fundamental third-sound resonance corresponds to a wavelength twice the internal length of the cell. The amplitude of the resultant temperature oscillation, seen at the thermometer, depends not only on resonance but also on the thermal boundary resistance at the inner wall of the cell. One end of the cell, near the heater, is thermally grounded to the mixing chamber of a dilution refrigerator. A carbon paint thermometer, used to measure the cell temperature and detect third sound, spans the width of the cell at the opposite end. A thin Nichrome film evaporated across the width of the cell about 3 mm from the thermal ground serves as a third-sound generating heater. Opposite one another on the inside surfaces of the cell are two 2000 Å thick aluminum capacitor plates.

The cell is constructed from two sheets of optically smooth, 0.7 cm$\times$2.0 cm$\times$100 μm vitreous quartz. First, the hole for the electrical feedthrough to the capacitor plate is burned through each quartz sheet by focusing a $\frac{1}{150}$-sec, 3-W pulse from a CO_2 laser on the sheet. The aluminum dot and the rectangular plate are then evaporated on each sheet. During these evaporations enough aluminum strays into the hole from each side to form an electrically continuous path from dot to plate. Approximately 1500 Å of SiO is evaporated over one plate to prevent the plates shorting together. The edges of the sheets are melted together to form an envelope-shaped cell with an inside separation of about 10 μm.[10] About 600 Torr of argon gas is admitted through the feedthroughs and trapped in the cell by filling the feedthroughs with epoxy. Finally, the heater, thermometer, and electrical leads are attached, and the completed cell is mounted inside a vacuum can attached to a dilution refrigerator.

The helium required to form the film is admitted to the vacuum can surrounding the cell, and it diffuses into the cell through the quartz walls at room temperature. Charging the cell with helium takes 24 h. Because the triple point for argon lies at a pressure of 517.2 Torr and a temperature of 83.8 K, the argon sublimes onto the cell walls when the cell is cooled to about 70 K. Below 30 K, the helium film begins to condense.

The cell provides a method of measuring vapor pressure unobscured by thermomolecular effects. As the pressure difference between outside and inside the cell, P, changes, the spacing between the walls of the cell changes: the capacitance between the plates, C, can then be used to indicate the pressure

$$P=\eta\frac{C_0-C}{C}\ , \tag{1}$$

where C_0 is the capacitance when $P=0$ and η is the sensitivity. By applying external pressures at 4.2 K and measuring ΔC, the linear relationship between P and ΔC is verified and η determined. The constant η is typically 2×10^{-4} Torr/ppm. Since a ΔC of 0.1 ppm can be resolved with a standard three-terminal capacitance bridge, the pressure sensitivity of this technique is of order 10^{-5} Torr. Measurements of the ^{4}He-vapor pressure by this capacitance technique were used to determine the film coverages. Below about 0.65 K, the vapor pressure of a thin ^{4}He film is less than the pressure sensitivity of the cell. By measuring C_0 below 0.65 K and extrapolating to about 0.9 K, the small temperature dependence of C_0 can be subtracted from the data and the vapor pressure obtained using Eq. (1). The vapor pressure is related to the film coverage through the Frenkel-Halsey-Hill model[11]

$$\ln\left[\frac{P_0}{P}\right]=\frac{A}{T\sigma^3}\ ,$$

where P_0 is the bulk liquid vapor pressure, A is a van der Waals constant, known from Ref. 8, and σ is the ^{4}He coverage. The Frenkel-Halsey-Hill model provides film coverages in good agreement with low-temperature third-sound velocity.[12] This procedure provides measurements of the film thickness that are accurate to 5%.

III. RESONANCE LINE-SHAPE MEASUREMENTS

Using a two channel, lock-in amplifier both the thermal response of the cell in phase with the ac heater power (real part) and 90° out of phase (imaginary part) can be measured. A phase shift δ relative to the heater is present due to nonresonant processes such as phase lags produced by generating and detecting third-sound temperature waves through the thin quartz walls of the cell. Dividing the change of the thermometer resistance by the thermometer sensitivity results in a plot of R vs T, the result is a plot of the phase and amplitude of temperature oscillations at the cell thermometer, $T_R(\omega)$, as a function of excitation frequency such as shown in Fig. 2. If Z_0, the nonresonant background, as well as δ were zero then, for a linear, Lorentzian resonance

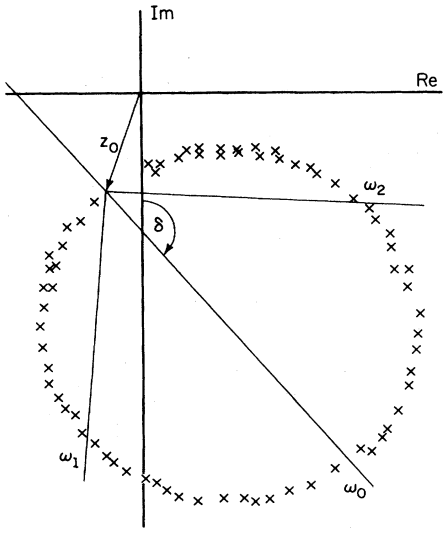

FIG. 2. A parametric plot of the in-phase versus out-of-phase (with the heat pulses) signal from a third-sound resonance as the pulse frequency is varied from well below to well above the resonance. This method of analysis allows the determination of background, and phase shift as well as linewidth and resonant frequency.

$$|\omega T_R(\omega)| = \omega_0 T_R(\omega_0)\sin\phi \tag{2a}$$

and

$$\sin\phi = \frac{\gamma\omega}{[(\omega_0^2-\omega^2)^2+\gamma^2\omega^2]^{1/2}} . \tag{2b}$$

Equation (2a) represents a circle with diameter $\omega_0 T_R(\omega_0)$ tangent to the real axis and symmetric about the imaginary axis. If the data, as shown in Fig. 2, do not form a circle then the system is being overdriven and the ac heater power must be reduced. The resonant frequency ω_0 is determined by the intersection of the symmetry axis and the circle. The square of the resonance amplitude is reduced to half its maximum value when $\phi=\pi/4$ or $\phi=3\pi/4$, corresponding to the frequencies ω_1 and ω_2, given by the intersection of the circle and the 45° lines with respect to the symmetry axis. For narrow lines, these frequencies allow the Q to be calculated,

$$Q = \frac{\omega_0}{\omega_2-\omega_1} . \tag{3}$$

As the cell is cooled below the onset temperature for third-sound propagation the Q rapidly increases and then saturates near 10^4, as shown in Fig. 3. We at first thought this to be instrumental. However, further measurements, using a high-stability signal generator, have convinced us that it is a fundamental line broadening within the superfluid phase. In the next section we will show how the signal strength, defined by

$$S = \frac{T_R(\omega_0)}{P_H} , \tag{4}$$

where P_H is the heater power, and Q are related to K_B and a second dissipation mechanism.

Since a small error in temperature can produce a large error in dR/dT of the thermometer and since, to avoid nonlinearities in the resonance a minimum of heater power had to be used, the overall uncertainty in the oscillator strength discussed is 45%. Our raw data include the Q *versus* T shown in Fig. 3 and S *versus* T shown in Fig. 4. The units of helium film coverage are atomic layers where one atomic layer corresponds to 7.8×10^{14} atoms/cm^2.

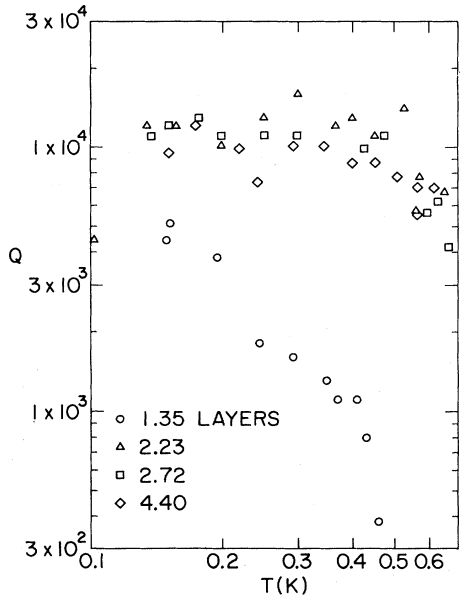

FIG. 3. The Q, $F_0/\Delta F$, is plotted versus temperature for various film thicknesses. The Q saturates at 10^4 to become independent of film thickness and temperature. This effect can be interpreted as due to $T=0$ surface friction.

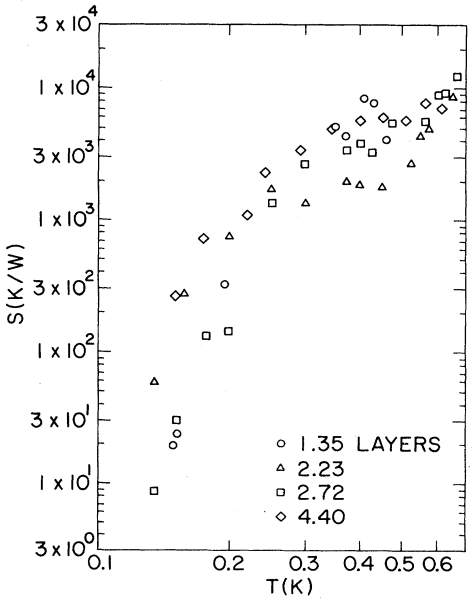

FIG. 4. The strength, S, of the resonance versus temperature. Note the rapid drop with decreasing temperature. S, which represents our "raw" data, has the effects of both linewidth and heater power removed. The qualitative behavior of S is reflected in the final result for the boundary conductance, K_B.

IV. THERMAL MODEL

This section first presents a thermal model that relates oscillator strength [Eq. (4)], heater power, and Q [Eq. (3)] to the properties of the film and substrate. To obtain a quantitative estimate of the thermal boundary resistance we must solve, simultaneously, for both the third-sound wave in the helium film and the diffusive wave in the quartz substrate.

Third sound is a traveling wave in T_f, the temperature of the film; σ_s, the superfluid areal density; σ, the liquid areal density (at $T=0$, $\sigma_s=\sigma$); and T_Q, the temperature of the substrate. For analysis of the model cell, these four quantities depend on only one spatial coordinate and time. The model cell is shown in Fig. 5, and the coordinate system is defined there. The heater generates a wave front that travels from the heater, along the length of the cell, and back to the heater via the other sheet. If the wave front returns in phase with the heater, resonance is established. Clearly this motion can be described with only one coordinate in the plane of the sheet, x, the distance from the heater along the major perimeter of the cell. For the thin films studied, T_f, σ, and σ_s do not depend on distances perpendicular to the substrate. Monolayer helium films are described by macroscopic quantities that do not vary with the distance from the substrate.[13] The substrate temperature T_Q is independent of the perpendicular distance from the film-substrate interface because the substrate is thinner than a thermal wavelength. If the temperature at the film-substrate interface varies harmonically at frequency ω,

$$T(0,t)=T_0e^{-i\omega t},$$

a solution of the diffusion equation,

$$C\frac{\partial T}{\partial t}=K\frac{\partial^2 T}{\partial_z 2},$$

where z is the distance from the film-substrate interface, C is the heat capacity per unit length (for the area of the sheet) along z, and K is the thermal conductance in the z direction, is

$$T(z,t)=T_0e^{-i\omega t}\exp\left[i\left[\frac{\omega C}{2K}\right]^{1/2}z\right]\times\exp\left[-\left[\frac{\omega C}{2K}\right]^{1/2}z\right].$$

For the frequencies used in this experiment and from the values of C and K calculated from the specific-heat and thermal-conductivity data given by Stephens,[9] the thermal wavelength, defined by

$$\lambda\equiv\left[\frac{2K}{\omega C}\right]^{1/2},$$

is at least 10 times the thickness of the cell wall. Therefore, variations in T_Q perpendicular to the film are negligible. The three differential equations that relate T_f, T_Q, σ_s, and σ must be solved subject to boundary conditions imposed by the geometry of the cell.

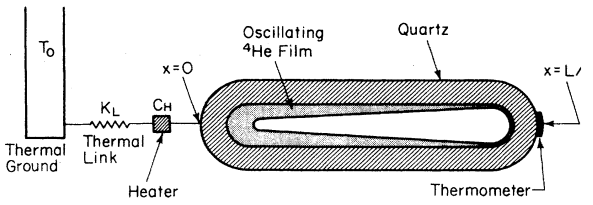

FIG. 5. The thermal model for the third-sound resonator shown in Fig. 1 and developed in Sec. IV.

Two equations are the result of applying two-fluid hydrodynamics. For a thin film in the one-dimensional cell, the usual equation of motion for the superfluid[14–16] becomes

$$m\frac{\partial v_s}{\partial t}=-\frac{\partial\mu}{\partial x}-m\Gamma v_s, \tag{5}$$

where m is the mass of the ^{4}He atom, v_s is the superfluid velocity, and μ is the chemical potential. The second term on the right is surprising but is needed to saturate Q and must be proportional to v_s in order to provide the Lorentzian line shape seen in Fig. 2. Formally, Γ can be equated to ζ_3k^2 in formula 9-16 of Khalatnikov[16] where k is the wave number for third sound. ζ_3 is the only important coefficient of second viscosity for deceleration of a moving superfluid if the normal flow velocity is maintained at zero (as is our case). We shall discuss this term later. In a thin film, the normal fluid cannot move because the film is thinner than the viscous penetration length of the normal fluid.[5] This has two consequences. First, the conservation of mass equation becomes

$$\frac{\partial\sigma}{\partial t}=-\sigma_s\frac{\partial v_s}{\partial x}, \tag{6}$$

and second, there can be no variation in the entropy density of the film, S_f, due to fluid flow, because the entropy is trapped in the motionless normal component. Changes in S_f can take place, however, if heat flows through the boundary conductance, K_B, between the film and substrate:

$$\frac{\partial S_f}{\partial t}=\frac{K_B}{T_f}(T_Q-T_f). \tag{7}$$

Second-order terms have been dropped from Eqs. (5), (6), and (7). Equations (5) and (6) can be combined by eliminating v_s, and when μ and S_f are written in terms of T_f and σ, the equations for the film become

$$\frac{\partial^2\sigma}{\partial t^2}=\frac{\sigma_s}{m}\left[\frac{\partial\mu}{\partial\sigma}\bigg|_{T_f}\frac{\partial^2\sigma}{\partial x^2}+\frac{\partial\mu}{\partial T_f}\bigg|_{\sigma}\frac{\partial^2 T_f}{\partial x^2}\right]-\Gamma\frac{\partial\sigma}{\partial t} \tag{8}$$

and

$$\frac{\partial S_f}{\partial\sigma}\bigg|_{T_f}\frac{\partial\sigma}{\partial t}+\frac{\partial S_f}{\partial T_f}\bigg|_{\sigma}\frac{\partial T_f}{\partial t}=\frac{K_B}{T_f}(T_Q-T_f). \tag{9}$$

The equation for T_Q is the one-dimensional diffusion equation with an additional term due to heat flow into the substrate from the film:

$$C_Q\frac{\partial T_Q}{\partial t}=K_Q\frac{\partial^2 T_Q}{\partial x^2}+K_B(T_f-T_Q)\ . \tag{10}$$

Here C_Q is the substrate heat capacity per unit length along x, K_Q is the thermal conductance of the cell wall parallel to x, and K_B is the boundary conductance per unit length.

The boundary conditions are chosen as follows. At the heater, $x=0$, and at the opposite end of the cell, $x=L/2$, the gradient of T_f vanishes by symmetry:

$$\left.\frac{\partial T_f}{\partial x}\right|_{x=0}=\left.\frac{\partial T_f}{\partial x}\right|_{x=L/2}=0\ . \tag{11}$$

At $x=L/2$, a third boundary condition is

$$\left.\frac{\partial T_Q}{\partial x}\right|_{x=L/2}=0\ . \tag{12}$$

Because in the model the heater and thermal link to the bath act at the point $x=0$, there is a cusp in T_Q at $x=0$ that is proportional to P_Q, the power flowing down the cell wall from the heater:

$$\left.\frac{\partial T_Q}{\partial x}\right|_{x=0^+}=-\frac{P_Q}{2K_Q}\ . \tag{13}$$

A fifth boundary condition is provided by

$$P=P_Q+C_H\left.\frac{\partial T_Q}{\partial t}\right|_{x=0}+K_L[T_Q(0,t)-T_0]\ . \tag{14}$$

P is the heater power, C_H is the heat capacity of the heater, and K_L is the thermal conductance of the link to the heat reservoir at temperature T_0.

The first step in the solution of the cell model is to linearize Eqs. (7)—(9). The primed variables σ', T_f', T_Q' are the small ac amplitudes, at frequency ω, of σ, T_f, T_Q, respectively. The wave vector k may be complex. We obtain

$$-\omega^2\sigma'+c_T^2k^2\sigma'-i\Gamma\omega\sigma'+ak^2T_f'=0\ , \tag{15}$$

$$-i\omega b\sigma'-i\omega C_\sigma T_f'-K_B(T_Q'-T_f')=0\ , \tag{16}$$

and

$$-i\omega C_Q T_Q'+k^2K_Q T_Q'+K_B(T_f'-T_Q')=0\ , \tag{17}$$

where

$$c_T^2=\frac{\sigma_s}{m}\left.\frac{\partial\mu}{\partial\sigma}\right|_{T_f}\ , \tag{18}$$

$$a=\frac{\sigma_s}{m}\left.\frac{\partial\mu}{\partial T_f}\right|_{\sigma}\ , \tag{19}$$

$$b=T_0\left.\frac{\partial S_f}{\partial\sigma}\right|_{T_f}\ , \tag{20}$$

and

$$C_\sigma=T_0\left.\frac{\partial S_f}{\partial T_f}\right|_{\sigma}\ . \tag{21}$$

The quantity c_S is defined by

$$c_S^2=c_T^2-\frac{ab}{C_\sigma}\ . \tag{22}$$

The velocities c_T and c_S are analogous to the isothermal and adiabatic sound velocities in a gas. The definition of c_T,

$$c_T^2=\frac{\sigma_s}{m}\left.\frac{\partial\mu}{\partial\sigma}\right|_{T_f}\ ,$$

is in the form of an areal density times a two-dimensional isothermal compressibility. Using the definitions of a, b, and C_σ, the definition of c_S can be rewritten as

$$c_S^2=\frac{\sigma_s}{m}\left.\frac{\partial\mu}{\partial\sigma}\right|_{T_f}-\left.\frac{\partial\mu}{\partial T_f}\right|_{\sigma}\frac{\left.\frac{\partial S_f}{\partial\sigma}\right|_{T_f}}{\left.\frac{\partial S_f}{\partial T_f}\right|_{\sigma}}\ .$$

Using a standard partial differential theorem and

$$\left.\frac{\partial\mu}{\partial\sigma}\right|_{s_f}=\left.\frac{\partial\mu}{\partial\sigma}\right|_{T_f}+\left.\frac{\partial\mu}{\partial T_f}\right|_{\sigma}\left.\frac{\partial T_f}{\partial\sigma}\right|_{s_f}\ ,$$

we obtain

$$c_S^2=\frac{\sigma_s}{m}\left.\frac{\partial\mu}{\partial\sigma}\right|_{s_f}\ ,$$

establishing c_S (as an adiabatic sound velocity).

Equation (15) is solved for σ' and the result substituted into Eq. (16). This results in two coupled equations for T_f' and T_Q' which can be written in matrix form as

$$\begin{bmatrix} i\omega C_\sigma(\omega^2+i\Gamma\omega-c_s^2k^2)-K_B(\omega^2+i\Gamma\omega-c_T^2k^2) & K_B(\omega^2+i\Gamma\omega-c_T^2k^2) \\ K_B & (i\omega C_Q-K_Qk^2)-K_B \end{bmatrix}\cdot\begin{bmatrix}(T_f')\\(T_Q')\end{bmatrix}=0\ . \tag{23}$$

Setting the determinant of the matrix to zero provides quadratic equations for k^2. The two roots describe a damped third-sound wave and a modified diffusive wave. The third-sound wave vector is approximately

$$k_T^2(\omega)=\frac{\omega^2[\omega C_\sigma C_Q+iK_B(C_\sigma+C_Q)](1+i\Gamma/\omega)}{\omega C_\sigma C_Q c_s^2+iK_B(C_Q c_T^2+C_\sigma c_s^2)}\ . \tag{24}$$

Notice that when $K_B=0=\Gamma$, the mode is adiabatic third

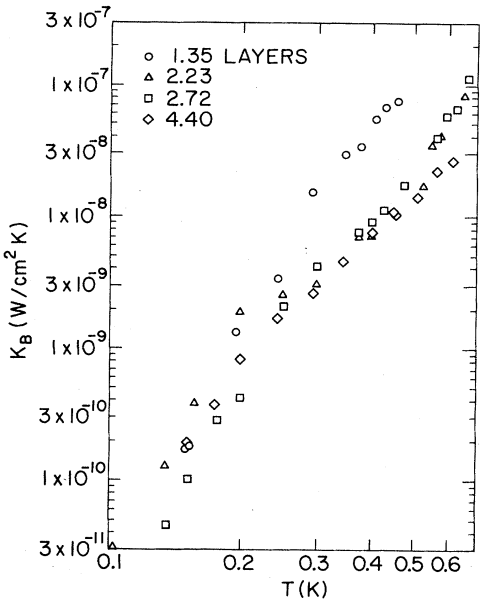

FIG. 6. From the analysis of the data, the boundary conductance K_B versus temperature is shown for various film thicknesses. A least-squares power-law fit produces $0.25 \times 10^{-4} T^{6.53\pm1.0}$ W/cm^{2}K.

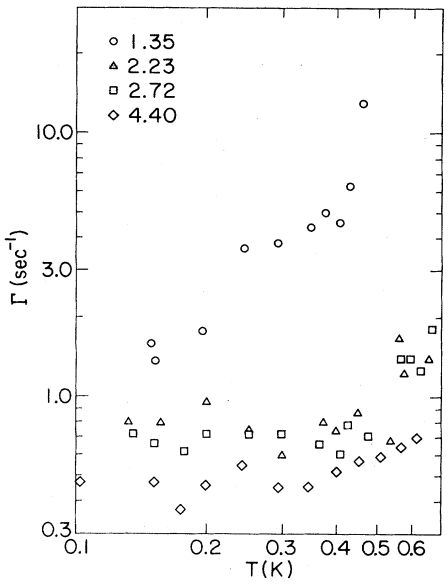

FIG. 7. The phenomenological parameter Γ, introduced to account for the saturation of the Q at low temperatures, versus temperature. Since the product of Γ and the superfluid coverage is roughly constant, Γ can be interpreted as a surface friction.

sound, and finite Γ gives a damped third-sound wave. After the wave vectors are found, the ratio of T_f' to T_Q' can be calculated for each mode. Using the subscript I for the third sound mode and II for the diffusive mode the results are approximately

$$\frac{T'_{f\mathrm{I}}}{T'_{Q\mathrm{I}}} \equiv \alpha \cong \frac{K_B - i\omega C_Q}{K_B} \tag{25}$$

and

$$\frac{T'_{f\mathrm{II}}}{T'_{Q\mathrm{II}}} \equiv \beta \cong \frac{K_B}{K_B - i\omega C_\sigma} . \tag{26}$$

For small K_B, the third-sound temperature oscillations are large in the film and small in the substrate, and conversely for the diffusive mode, as one would expect.

Linear combinations of the modes that satisfy the boundary conditions, Eqs. (11)—(14), form the solution of the problem. The temperature oscillations in the quartz are

$$T'_Q(x) = \frac{P_Q}{2K_Q}\frac{\beta}{ik_{\mathrm{I}}(\beta-\alpha)}\left[e^{ik_{\mathrm{I}}x}\frac{e^{-ik_{\mathrm{I}}(L/2)}}{e^{ik_{\mathrm{I}}(L/2)}-e^{-ik_{\mathrm{I}}(L/2)}} + e^{-ik_{\mathrm{I}}x}\frac{e^{ik_{\mathrm{I}}(L/2)}}{e^{ik_{\mathrm{I}}(L/2)}-e^{-ik_{\mathrm{I}}(L/2)}}\right]$$
$$+ \frac{P_Q}{2K_Q}\frac{\alpha}{ik_{\mathrm{II}}(\alpha-\beta)}\left[e^{ik_{\mathrm{II}}x}\frac{e^{-ik_{\mathrm{II}}(L/2)}}{e^{ik_{\mathrm{II}}(L/2)}-e^{-ik_{\mathrm{II}}(L/2)}} + e^{-ik_{\mathrm{II}}x}\frac{e^{ik_{\mathrm{II}}(L/2)}}{e^{ik_{\mathrm{II}}(L/2)}-e^{-ik_{\mathrm{II}}(L/2)}}\right] . \tag{27}$$

P_Q is obtained from Eq. (14) with Eq. (27) evaluated at $x=0$ substituted for $T_Q(0,t)-T_0$.

When $\mathrm{Im}\,k_{\mathrm{I}}$ is small, the first term of Eq. (27) is very nearly a Lorentzian resonance,

$$T'_{Q\,\mathrm{res}} = \frac{P_Q}{K_Q}\frac{\beta}{\beta-\alpha}\frac{c_s^2}{L}\frac{2}{\omega^2-\omega_0^2+2ic_s\mathrm{Im}(k_{\mathrm{I}})} . \tag{28}$$

We see

$$Q = \frac{\omega_0}{2c\,\mathrm{Im}(k_{\mathrm{I}})} . \tag{29}$$

The approximate expression, Eq. (28), agrees with the exact expression, Eq. (27), to within 5%.

V. DATA ANALYSIS

The thermal model allows us to calculate S and Q as functions of four parameters, K_B, Γ, K_L, and C_H. The value of K_L was chosen to be equal to the thermal conductivity of 1 cm of vitreous quartz cell wall. This value also takes into account the epoxy joint between the cell and the copper heat sink. The heat capacity of the heater was chosen to be the heat capacity of 0.06 cm of cell wall, the size of the actual heater. Increasing C_H by a factor of 2 and decreasing K_L by a factor of 10 changed the value of K_B derived from the model by 30% and the value of Γ by 3% at most. The thermal conductivity and heat capacity of vitreous quartz were taken from Stephens.[9] The values of c_S, c_T, and C_σ were calculated from the two-

dimensional thermodynamics described in Ref. 13.

Measurements of Q and S for four helium films are shown in Figs. 3 and 4. The film thicknesses range from 1.35 total atomic layers to 4.40 total layers, well within the thickness domain of two-dimensional excitations. A computer program was written that accepted trial values of K_B and Γ, calculated the necessary thermodynamic functions, solved the exact expressions for $k_{\rm I}$, $k_{\rm II}$, α, β, and finally calculated S by dividing $T'_Q(L/2)$ from Eq. (27) by P from Eq. (14). The program calculated Q from the approximation Eq. (29). The values of K_B and Γ needed to fit the data are unique and are shown in Figs. 6 and 7, respectively.

VI. DISCUSSION

This experiment shows that the dissipation of third sound below the onset temperature is due to at least two causes. The finite thermal boundary conductance provides an extrinsic dissipation mechanism. As in earlier work[15] this mechanism is too weak to account for all of the dissipation, especially at low temperatures. For example, if K_B were responsible for all of the dissipation our thermal model predicts Q values 2—3 orders of magnitude larger than those measured near 0.1 K. At the temperatures and film coverages spanned by these measurements, the other thermal channel through the gas[17] is entirely negligible. This forces the inclusion of an intrinsic dissipation mechanism which we have parametrized in Eq. (5).

In the usual Kapitza conductance problem between solids and bulk liquid helium, the measured Kapitza conductance is typically a factor of roughly 50 larger at 0.1 K than the conductance calculated from the Khalatnikov model.[16] A power-law least-squares fit to our results produces

$$K_B = 0.25 \times 10^{-4} T^{6.3\pm1.0}\ \mathrm{W/cm^2\,K}\ .$$

In contrast to the bulk case the thin-film boundary conductance is 4 orders of magnitude smaller than the Khalatnikov result at 0.1 K and has a much stronger temperature dependence. Clearly the processes that carry the heat in the Khalatnikov model are completely suppressed by the restricted dimensionality of the film.

Since the two-phonon processes in the Khalatnikov model are eliminated by the two-dimensional nature of the excitations in the film, it is reasonable to try three-phonon processes next. An example of such a process could be a substrate phonon striking the surface to produce a reflected phonon and an excitation in the helium film. The phenomenology of Lumpkin and Saslow[4] for a solid radiating into bulk helium gives a three-phonon transmission coefficient of T^6 and a boundary conductance which varies as T^9. However, for a thin helium film, the normal component cannot be excited. For this case the boundary conductance will vary as T^7 which is consistent with what we observe. Presently, it is not possible to calculate a magnitude from this work. Rutledge, McMillan, and Mochel[18] have estimated the magnitude of K_B due to one three-phonon process and finds that K_B is very sensitive to the velocity of sound in the substrate. Interestingly, in order to make the magnitude of the calculated three-phonon K_B large enough one must use a slow sound velocity, like the sound velocity in solid ^{4}He, for the phonon velocity in the substrate.

In the usual Kapitza problem most of the heat is transported by an anomalous mechanism that allows phonons to carry heat that are forbidden to do so in the Khalatnikov model. The two dimensionality of the excitations in a thin ^{4}He film guarantees that the entire heat flow must be anomalous. Any of the mechanisms that have been used to explain the anomalous part of the bulk Kapitza conductance may be responsible for the conductance we measure. Many of the models require detailed knowledge of the helium-substrate interface that is difficult to obtain to make quantitative estimates of the size of the conductance. From this point of view it is not difficult to outline models that yield a temperature dependence close to $T^{6.3\pm1.0}$. In the presence of roughness or surface states conservation of momentum parallel to the interface would be relaxed. If a temperature-independent transmission coefficient is assumed, the resulting temperature dependence of K_B is T^4 for excitations in the film with a linear dispersion. If one includes the full excitation dispersion[13] the temperature dependence lies between T^4 and $T^{4.5}$ depending on the film thickness. Now all one needs to do is to invoke a temperature-dependent phonon transmission coefficient. Kinder[19] has shown that glasslike surface defects would give a phonon transmission coefficient proportional to T, or the frozen layer may provide a coupling mechanism. It is expected, due to freezing and melting between liquid and solid helium, that phonon coupling between these phases of helium will vary as ω^2 due to interface curvature. In our case, with thermal phonons, this would lead to an additional T^2 temperature dependence. Involving the frozen layer of helium in this fashion is what the numbers indicated should be done in the McMillan model discussed above. It would then be expected that the boundary conductance would be quite sensitive to ^{3}He which can block the rapid freezing and melting. However, ^{3}He would also increase the density of states in the helium film. In fact, we see experimentally that ^{3}He does enhance the boundary conductance. We are presently exploring this behavior.

It is possible to place a crude physical interpretation on Γ, the damping term invoked to account for the saturation of the measured Q. Using the results for helium on argon obtained in Ref. 13, we have an inert helium layer with an average thickness of one atomic layer to subtract from the net film thickness to obtain the mean superfluid thickness. If we multiply Γ by this superfluid film thickness we obtain a result roughly independent of film thickness, a Γd_s of 1.0 atomic layers/sec. This can be interpreted as a surface friction which is present for the flow of superfluid even in the limit of $T=0$. It has also been pointed out[20] that if Γ can be compared to Khalatnikov's[16] second viscosity, ζ_3, then Γ should increase as k^2. This is being checked. Pinned vortex pairs could produce such behavior—although we have not found this behavior to be sensitive to substrates.

In summary, even the qualitative thermal behavior of thin helium films shown in Fig. 3 below 0.7 K indicates

behavior distinct from bulk processes. An analysis of these results produces a boundary conductance $K=0.25\times10^{-4}T^{6.3\pm1.0}$ W/cm^{2}K. This boundary conductance, below 0.1 K, can become so small that such a flowing helium film could become substantially hotter than its substrate. To our knowledge this is the first measurement of boundary resistance to a two-dimensional superfluid. There is a second dissipation process that dominates at low temperatures. We have included the effect of this process as a force term in Eq. (5). The force on the superfluid is independent of the film thickness and proportional to v_s.

ACKNOWLEDGMENTS

We would like to acknowledge the help of A. L. Buck in establishing that our line broadening was not due to oscillator drift. Professor W. L. McMillan provided substantial help in our attempt to understand the experimental result. We would also like to thank W. M. Saslow for some valuable comments which we have included in the final draft. We also gratefully acknowledge the support of the National Science Foundation through Grants Nos. NSF DMR81-13487 and NSF DMR77-23999.

---

*Present address: Physics Department, University of California at Irvine, Irvine, CA 92717.

[1]For a review of this subject, see A. C. Anderson, in *Phonon Scattering in Solids,* edited by L. J. Challis, V. W. Rampton, and A. F. G. Wyatt (Plenum, New York, 1976).

[2]H. W. M. Salemink, H. van Kempen, and P. Wyder, J. Phys. C **13**, 5089 (1980). This experiment directly examines phonon transmission, with mode conversion, in bulk helium. Their discussion also contains an excellent review of earlier investigations.

[3]J. Weber, W. Sandmann, W. Dietsche, and H. Kinder, Phys. Rev. Lett. **40**, 1469 (1978).

[4]M. E. Lumpkin and W. M. Saslow, Phys. Rev. B **20**, 1035 (1979).

[5]K. R. Atkins and I. Rudnick, in *Progress in Low Temperature Physics,* edited by C. J. Gorter (North-Holland, Amsterdam, 1964), Vol. VI, Chap. 2; B. Ratnam and J. Mochel, J. Low Temp. Phys. **3**, 239 (1970).

[6]C. Guo and H. J. Maris, Phys. Rev. Lett. **29**, 855 (1972).

[7]G. N. Crisp, R. A. Sherlock, and A. F. G. Wyatt, in *Proceedings of the 14th International Conference on Low Temperature Physics, Otaniemi, Finland, 1975,* edited by Matti Krusius and Matti Vuori (North-Holland, Amsterdam, 1975), Vol. 1, pp. 455–458.

[8]E. S. Sabisky and C. H. Anderson, Phys. Rev. A **7**, 790 (1973).

[9]R. B. Stephens, Phys. Rev. B **13**, 852 (1976).

[10]B. A. Ratnam, Ph.D. thesis, Univeristy of Illinois, 1972.

[11]D. M. Young and A. D. Crowell, *Physical Adsorption of Gases* (Butterworths, Washington, 1962).

[12]J. H. Scholtz, E. O. McLean, and I. Rudnick, Phys. Rev. Lett. **32**, 147 (1974); T. E. Washburn, J. E. Rutledge, and J. M. Mochel, *ibid.* **34**, 183 (1975).

[13]J. E. Rutledge, W. L. McMillan, J. M. Mochel, and T. E. Washburn, Phys. Rev. B **18**, 2155 (1978).

[14]J. Wilks, *The Properties of Liquid and Solid Helium* (Clarendon, Oxford, 1967).

[15]J. E. Rutledge, Ph.D. thesis, University of Illinois, 1978.

[16]I. M. Khalatnikov, in *Introduction to the Theory of Superfluidity,* edited by D. Pines (Benjamin, New York, 1965), Chap. 23, pp. 146.

[17]H. Schubert, P. Leiderer, and H. Kinder, J. Low Temp. **39**, 363 (1980).

[18]J. E. Rutledge, W. L. McMillan, and J. M. Mochel, *Proceedings of the 16th International Conference on Low Temperature Physics* [Physica **108B&C**, 401 (1981)].

[19]H. Kinder, Physica **107B**, 549 (1981).

[20]W. M. Saslow (private communication).